OPEN

Silicon reduces the iron uptake in rice and induces iron homeostasis related genes

Martin Becker [1,2*], Ngoc Sang Ngo[1] & Manfred Karl Adolf Schenk[1]

Gramineous plants take up silicon (Si) that enhances the formation of exodermal Casparian bands (CBs) in the roots of rice (*Oryza sativa* L.). Furthermore, it is known that Si supply reduces the concentration of Fe in rice shoots. We hypothesized that the Si-enhanced CB formation in the exodermis reduces in the flux of Fe in the apoplast and the uptake of Fe loaded deoxymugineic acid. Thus, the effect of silicic acid supply at varied Fe concentrations and Fe forms was investigated in nutrient solution. The Fe concentrations in the shoot and apoplastic Fe concentrations in the root were determined and an Affymetrix GeneChip experiment was carried out together with qRT-PCR measurements for observation of transcriptomic reactions. Additionally, the Fe uptake of an overexpression mutant of Os*ABCG25* with an enhanced exodermal CB formation was investigated. The application of silicic acid reduced the Fe concentrations in shoot DM independently of the supplied Fe concentration and Fe form. As a reaction to the Fe shortage, the full cascade of Fe-homeostasis-related genes in the roots was upregulated. Silicic acid supply also decreased the apoplastic Fe concentrations in roots. In addition, an overexpression mutant of Os*ABCG25* with an enhanced CB formation showed a reduced uptake of Fe in excess Fe conditions. The results suggest that the Si-induced CB formation in the exodermis hampers the flux of Fe into the apoplast of the cortex and, thus, Fe uptake of rice grown in nutrient solution which is reflected in the upregulation of Fe homeostasis-related genes.

Silicon (Si) is the second most abundant element in the soil crust and many plants can take up and accumulate Si[1–3] which has beneficial effects, such as a higher resistance to herbivores or powdery mildew, a higher drought resistance and a higher stability of the leaves[4]. Another effect of Si is the earlier formation of the exodermal Casparian bands (CBs) which appear in submerged grown rice[5,6]. The mechanism is not yet clear[7] but it is suggested that $Si(OH)_4$ forms crosslinks with phenols within cell walls leading to an enhanced CB development. The CBs are depositions of suberin and lignin in anticlinal cell walls of the endodermis of all higher plants and of the exodermis of many plants[8,9]. Endodermal CBs control the unselective bypass flow of water and ions into the vascular bundle[10]. Exodermal CBs are described in rice as controlling radial oxygen loss and water flux[11,12]. It is also indicated in the literature that the exodermal CBs could affect in nutrient acquisition. Due to the late occurrence of CBs during root development and the disruptions of the exodermis from lateral roots, it is mentioned that the effect of exodermal CBs in ion exchange should not be overestimated[13,14]. Accordingly, the flux of apoplastic tracer, such as trisodium 3-hydroxy-5,8,10-pyrene trisulfonat or cis-absicid acid was not hampered by the exodermal CBs[10,15]. But, the exodermal CBs are also described as a diffusion barrier reducing the flux of ions into the cortex[16–19] and to have a function in controlled substance exchange[20–22], while positive effects of the exodermal CBs for water management are also described[8]. Furthermore, it has been shown that Si supply reduces the bypass flow of sodium and, thus, the sodium uptake declines[17,18,23,24].

Rice has exodermal CBs which have a specific function regarding the aerenchyma, which is a root tissue developing from collapsing cortical cells to ensure the oxygen supply of the root[25,26]. Exodermal CBs block the radial oxygen loss in adventitious roots[6]. Previously it was shown that Si enhances the formation of exodermal CBs in adventitious roots of rice and clearly reduces the radial oxygen loss[6,27]. The exodermal CB formation starts with/ without Si application 4–5/8–10 cm from the root tip in the anticlinal cell walls and is completed at 7–8/12–13 cm distance from the root tip, respectively[6,28].

[1]Institute of Plant Nutrition, Faculty of Natural Sciences, Leibniz University Hannover, Herrenhäuser Str. 2, 30419, Hannover, Germany. [2]Present address: Leibniz Institute of Plant Genetics and Crop Plant Research (IPK), Plant Reproductive Biology; Corrensstr. 3; D-06466 Seeland/OT, Gatersleben, Germany. *email: becker@ipk-gatersleben.de
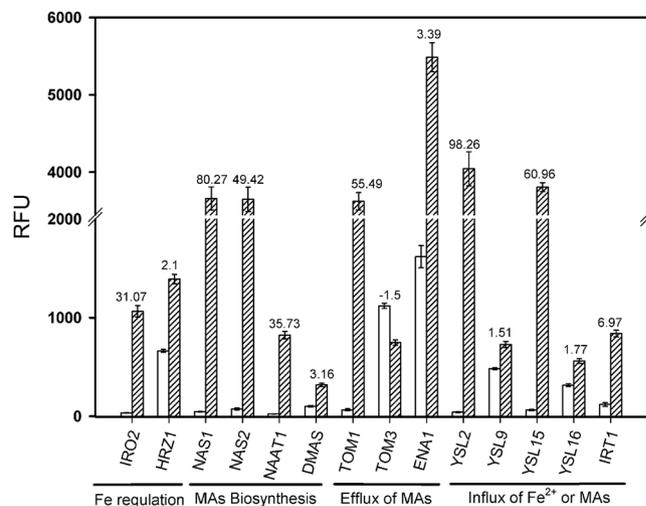
Figure 1. Regulation of Fe homeostasis-related genes through silicic acid (Si) in rice roots from the Affymetrix GeneChip experiment. Yellow dotted bars represent the Si-treated plants grown with Si (30 mg L^{-1}) in nutrient solution; blue bars represent plants grow. n with low Si concentrations (3 mg L^{-1}). The relative fluorescence unit (RFU) is shown; bars indicate the standard error (SE). Numbers above the bars represent the foldchange (FC). Abbreviations of the genes are: DMAS: Deoxymugineic acid synthase; ENA1: Efflux of nicotianamine 1; HRZ1: Haemerythrin motif-containing RING-& Zinc finger protein 1; IRO2: Iron-related transcription factor 2; IRT1: Iron related transporter 1; NAAT1: Nicotianamine aminotransferase 1; NAS1: Nicotianamine synthase 1; NAS2: Nicotianamine synthase 2; TOM1: Transporter of mugineic acid 1; TOM3: Transporter of mugineic acid 3; and YSL2/9/15/16: yellow stripe like (YSL) transporter 2/9/15/16.

Silicon also affects nutrient uptake in rice. Previous studies[27,29] reported that Si supply reduced the Fe uptake of plants grown in nutrient solution and under Fe excess the toxicity symptom leaf bronzing clearly decreased[30] but causal relationships are still not clear. Iron acquisition in plant kingdom follows two strategies[31]. In dicotyledonous and monocotyledonous non-graminaceous species (strategy I) Fe(III) precipitates are dissolved in the rhizosphere by release of protons and excreted phenols such as coumarins chelate Fe(III)[32]. This complex diffuses to the root surface where the membrane bound ferric reductase reduces Fe(III) to Fe(II) which is taken up by iron related transporter (IRT). The activity of the ferric reductase is enhanced by low pH. Graminaceous plants such as rice follow strategy II in Fe uptake[33]. In strategy II, plants secrete via TOM1 phytosiderophores, such as deoxymugineic acid (DMA), into the rhizosphere that bind to hardly available Fe^{III+}. This complex is taken up by yellow stripe-like (YSL) transporters at the root epidermis and, most probably, in the root cortex[34–36]. Under Fe deficiency iron homeostasis genes are regulated and the expression of genes involved in the synthesis of DMA from methionine such as nicotianamine synthase (NAS), nicotianamine aminotransferase (NAAT), and deoxymugineic acid synthase (DMAS) is enhanced. Also genes encoding for mugineic efflux transporters (TOM) and influx transporters of Fe chelates (YSL) are upregulated[37–41]. The rhizosphere is different in plants grown in nutrient solution to those grown in soil since the whole pot volume can be defined as rhizosphere, because of the high diffusion coefficient in water. Thus, DMA is extremely diluted and less effective for Fe acquisition. In nutrient solution, the binding to DMA and the subsequent uptake is discussed to take place in the apoplastic space of the cortex[42].

The aim of this work is to identify the reasons for the lower Fe content in the leaves of plants grown with Si. We hypothesize that the earlier CB formation in the exodermis reduces the amount of Fe in the apoplast and, thus, reduces the uptake of DMA-loaded Fe.

Results

Silicic acid induced differential gene expression. Rice plants were grown with high (+Si, 30 mg L^{-1}) or low Si (−Si, 3 mg L^{-1}) in nutrient solution for 28 d. The zone 2–6 cm from the tip of adventitious roots was harvested, since here CB development in the exodermis is clearly enhanced by Si supply[28], and an Affymetrix GeneChip was used to identify differentially regulated genes. We observed 172 upregulated and 207 downregulated genes due to Si treatment with a minimal fold change of 2 at a p-value cut-off of 0.01 (Supplementary Fig. S1). The complete GeneChip experiment can be found under GSE111019 (Gene Expression Omnibus). A list of the 50 most up- and downregulated Si-related genes is given in Supplementary Table S1a,b. Fourteen of the upregulated genes were related to the Fe homeostasis in rice (Fig. 1) such as the Fe-regulating transcription factors Os*IRO2* (LOC_Os01g72370.1) and Os*HRZ1* (LOC_Os01g49470.2).

Additionally, genes for the desoxymugineic acid (DMA) biosynthesis, such as nicotianamine synthase 1/2 (Os*NAS1*, LOC_Os03g19427.1; Os*NAS2* LOC_Os03g19420.2), nicotianamine aminotransferase 1 (Os*NAAT1*, LOC_Os02g20360.1) and deoxymugineic acid synthase (Os*DMAS*, LOC_Os03g13390.2) were upregulated while Os*NAS3* was not regulated differentially. The mugineic acid (MA) efflux transporter Os*TOM1* (LOC_Os11g04020.1) was similarly upregulated, while the expression level of Os*TOM3* was decreased. The
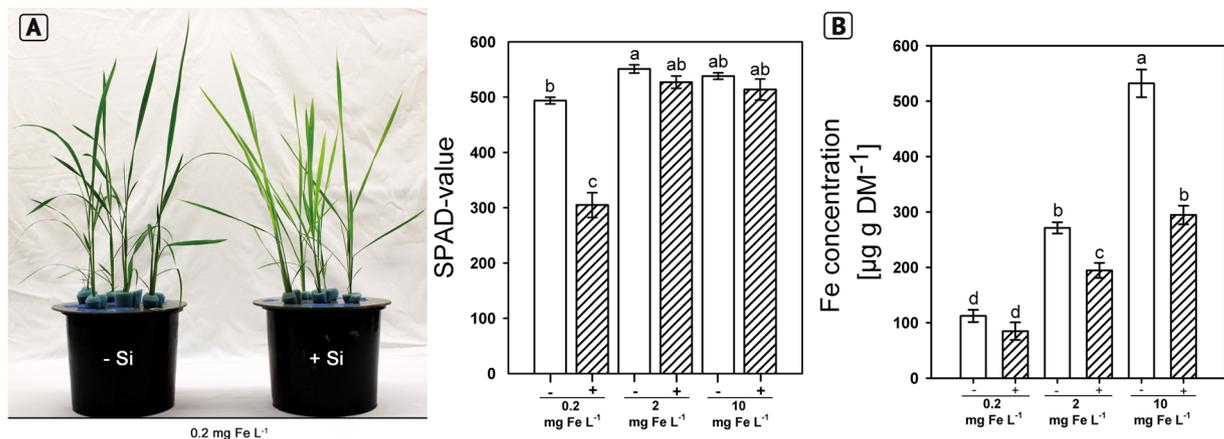
Figure 2. Iron nutritional status of rice plants grown in nutrient solution as affected by silicic acid supply (+Si: $30\,mg\,L^{-1}$, −Si: $3\,mg\,L^{-1}$) and Fe supply (Fe^{EDDHA}) **(A)** phenotypic differences between rice plants grown in low Fe conditions ($0.2\,mg\,L^{-1}$) and chlorophyll concentration of leaves shown as SPAD value of plants grown with low Fe ($0.2\,mg\,L^{-1}$), optimal Fe ($2\,mg\,L^{-1}$) and high Fe ($10\,mg\,L^{-1}$). **(B)** Iron concentrations in the shoot dry matter (DM). Ruled bars represent the +Si plants; white bars represent plants grown with −Si. Bars indicate the SE. Different letters indicate significant differences between treatments; Bonferroni test with $p < 0.05$.

nicotianamine efflux transporter Os*ENA1* responsible for Fe-MA mobilization in the vacuole was also upregulated. An increased expression level was furthermore observed for genes related to the influx of Fe-MA, such as Os*YSL2* (LOC_Os02g43370.2), Os*YSL9* (LOC_Os04g45860.1), Os*YSL15* (LOC_Os02g43410.2) and Os*YSL16* (LOC_Os04g45900.1). The Fe^{2+} transporter 1 (Os*IRT1*) was also upregulated. A differential regulation of genes involved in Fe-MA storage and sequestration was not observed (Os*Vit1.1/1.2*, LOC_Os04g38940.1/LOC_Os09g23300.1; Os*Fer1/2*, LOC_Os11g01530.1/LOC_Os12g01530.1).

Fe nutrition as affected by silicic acid at varied Fe supply. The observations suggested that Si supply induced a Fe shortage in rice plants. Thus, we investigated the Fe uptake and the gene expression as affected by Si nutrition at different Fe levels and Fe forms. Plants grown for 28 d in +Si at the lowest Fe supply showed Fe deficiency symptoms (Fig. 2A) compared to the other treatments, which was also reflected in the SPAD values (Fig. 2A). Furthermore, the Fe concentration in shoot DM was reduced by Si supply in all Fe levels and reduction varied between 25 and 32.4% at low and high Fe levels, respectively (Fig. 2B). The Fe concentration in shoot DM was in the $2\,mg\,Fe\,L^{-1}$ treatment in the range as reported for well supplied plants[31,43].

This Si(OH)$_4$ effect was not due to an interaction with iron in the nutrient solution since hydrodynamic diameter was not affected as determined by Zeta-potential measurement combined with phase-analysis light scattering technique (Supplementary Fig. S2).

Silicic acid supply also reduced the Fe concentrations in shoot DM independently of the Fe form, as can be seen in Fig. 3. The Si effect was much stronger for plants grown with Fe$^{(II)}$SO$_4$ than with Fe^{EDDHA} and Fe^{EDTA}. The Fe supply in the form of Fe$^{(II)}$SO$_4$ enhanced the Fe concentration in shoot DM by a factor of two compared to the Fe chelates.

There was no difference in the chlorophyll concentrations (SPAD) at harvest between treatments (Supplementary Fig. 3), but plantlets grown in +Si with Fe^{EDTA} or Fe$^{(II)}$SO$_4$ showed chlorotic leaves at the beginning of the experiment. This effect was not measurable with the SPAD meter due to the small leaf area of the plantlets.

Since silicic acid supply reduced the Fe concentration in shoot DM regardless of the level and the form of Fe supply, we assumed a common mechanism for this Si effect. We hypothesized that the Si-enhanced CB development in the exodermis[6,27] reduced the Fe flux into the root apoplast where Fe is thought to be bound by DMA and then taken up by YSL transporters. Therefore, the apoplastic Fe concentrations were determined (Fig. 4). They clearly increased with increasing Fe supply and were reduced by Si supply at the two higher Fe supply levels.

Additionally, an overexpression mutant of the gene Os*ABCG25* (LOC_Os10g30610.1) having an enhanced CB development in the exodermis was used and grown under excessive Fe supply to reinforce the hypothesis[27]. The overexpression mutant grown without Si contained clearly less Fe in shoot DM compared to WT (Fig. 5). The application of Si to WT plants affected the Fe concentration similarly, but the effect was only slightly visible in the mutant.

Gene expression as affected by silicic acid at varied Fe supply. Silicic acid supply hampered the Fe nutrition of rice and this was reflected in the expression of Fe homeostasis genes. About half of the genes investigated were upregulated at the lowest Fe level without Si supply (Fig. 6A), but not differentially expressed at the highest Fe level compared to the optimal level of $2\,mg\,L^{-1}$. The expression of the same genes which were upregulated in the treatment $0.2\,mg\,Fe\,L^{-1}$ were also enhanced in all Fe levels by Si supply and the expression declined with increasing Fe concentration in the nutrient solution: The transcription factors Os*IRO2* and Os*HRZ1*, the chelate synthesis genes Os*NAS1*, Os*NAS2*, Os*NAAT1* and Os*DMAS*, the DMA efflux transporter genes Os*TOM1*
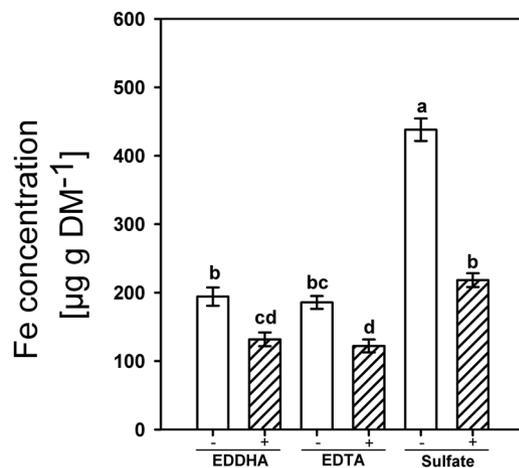
Figure 3. The Fe concentration in the shoot DM of rice as affected by the offered Fe form ($2\,mg\,L^{-1}$) and silicic acid supply ($+Si$: $30\,mg\,L^{-1}$, $-Si$: $3\,mg\,L^{-1}$) in nutrient solution. Ruled bars represent the $+Si$-treatments; white bars represent $-Si$ treatments. Bars indicate the SE. Different letters indicate significant differences between treatments; Bonferroni test with $p < 0.05$.
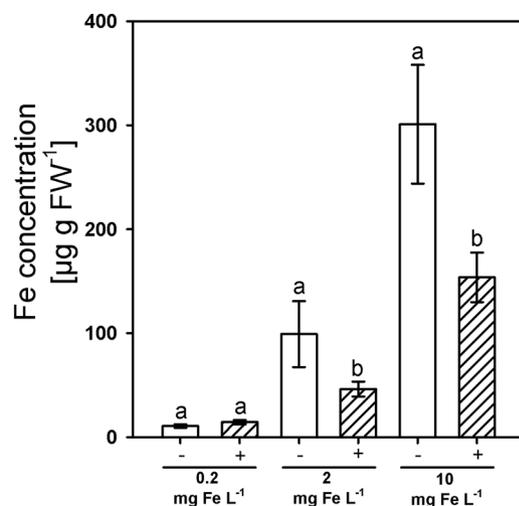

Figure 4. The Fe concentration in the apoplast of adventitious rice roots as affected by Fe supply (Fe^{EDDHA}) and silicic acid supply ($+Si$: $30\,mg\,L^{-1}$, $-Si$: $3\,mg\,L^{-1}$). Ruled bars represent $+Si$ plants; white bars represent $-Si$ plants. Bars indicate the SE. Different letters indicate significant differences between respective treatments; Wilcoxon rank sum test with $p < 0.05$.

and the Os*TOM3* homologon (*Os12g0132500*), and finally the Fe-MA uptake transporters YSL2 and YSL15. The expression of Os*ENA1* coding for a Fe-DMA/nicotianamine (NA) transporter from the vacuole was also enhanced.

A similar pattern of Si-induced gene expression was observed in the experiment with different Fe forms (Fig. 6B).

Discussion

Silicon reduced the concentration of Fe in the shoot of plants independently of the supplied Fe concentration and Fe form and triggered Fe deficiency symptoms (Figs. 2, 3). This agrees well with previous reports that Si supply decreases the Fe concentration in shoots of rice grown in nutrient solution[27]. Si supply also reduced the Fe concentration in shoot DM of rice grown in nutrient solution under Fe excess nutrition[44]. We further observed a reduction of the Fe concentration in the root apoplast (Fig. 4). Thus, we suggest that the Si-enhanced formation of the exodermal CBs led to a decrease of the Fe concentration in the apoplast and reduced Fe uptake.

The formation of exodermal CBs is promoted by Si and CBs occur earlier in the adventitious roots of rice[6] and in the roots of *Zea mays*, *Allium cepa*, *Tradescantia virginiana* and *Guizotia abyssinica*[28]. The endodermal CBs are well described to be an effective barrier for unselective bypass flow of substances from the apoplastic space into the vascular bundle[13,20,45,46] and the exodermal CBs were shown to hamper the flux of oxygen from
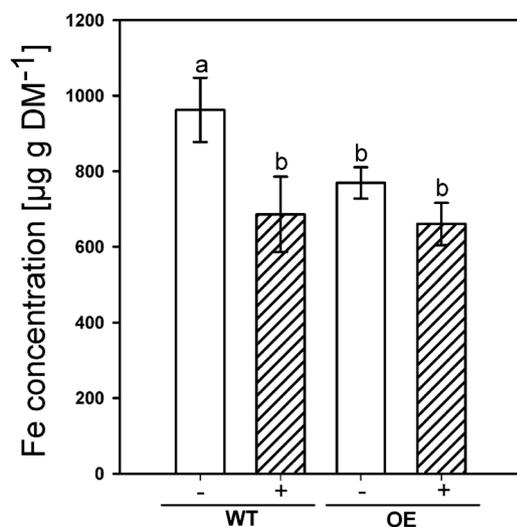
Figure 5. The Fe concentration in the shoot of WT and the overexpression mutant of OsABCG25 grown with excessive amounts of Fe ($250\,mg\,L^{-1}$ $FeSO_4$) in nutrient solution. Ruled bars represent the Si-treated plants (+Si, $30\,mg\,L^{-1}$); white bars represent plants grown with low Si (−Si, $3\,mg\,L^{-1}$) concentration. Bars indicate the SE. Different letters indicate significant differences between WT plants grown without Si (−WT) and other treatments; students t-test with $p < 0.05$.

A

Gene	0.2	10	0.2	2	10
IDEF1	1.03	0.82	1.39	1.09	1.04
IDEF2	1.20	0.62	1.38	1.53	1.06
Iro2	38.05*	0.83	107.63*	37.01*	10.48*
Hrz1	1.82	0.94	3.63*	2.60*	1.45
NAS1	24.65*	1.18	64.71*	15.89*	3.32
NAS2	342.51*	1.22	1552.09*	522.76*	24.93
NAS3	2.51*	1.00	2.41	0.68	0.31
NAAT1	91.14*	0.60	396.18*	148.06*	6.54*
DMAS	28.25	0.59	71.01*	7.67*	2.68*
ENA1	4.72*	0.68	7.94*	4.32*	1.62
ENA2	1.88	0.99	2.68	0.98	0.86
TOM1	93.70*	1.10	257.78*	115.36*	9.00*
TOM2	1.43	0.49	1.78	1.51	0.65
TOM3	0.78	0.87	1.17	1.89	1.72
TOM3_Homologon	88.03*	0.66	265.03*	82.14*	7.36
YSL2	374.81*	0.58	1160.07*	215.27*	22.63*
YSL6	1.04	0.55	1.51	1.79	0.98
YSL8	1.00	0.69	0.84	0.81	0.99
YSL13	1.40	0.50	2.83	1.49	0.95
YSL15	92.41*	0.14	178.53*	150.12*	33.59*
YSL16	1.84	0.35	1.85	2.62	1.89
	Minus Si		Plus Si		

B

Gene	EDTA	Sulfate	EDDHA	EDTA	Sulfate
IDEF1	0.13	0.69	1.16	1.16	0.68
IDEF2	0.02	0.50	0.64	0.64	0.44
Iro2	0.39	0.78	10.13*	20.82*	5.70
Hrz1	0.68	0.59	1.05	1.72	0.80
NAS1	0.94	0.85	1.90*	37.92*	5.44
NAS2	0.57	1.75	75.58*	144.01*	27.86*
NAS3	1.83	1.38	0.72	4.79	0.93
NAAT1	0.66	2.31	39.12*	125.37*	24.76*
DMAS	0.39	0.78	10.13	20.82	5.70
ENA1	0.27*	0.34*	0.75	1.59*	0.74
ENA2	0.68	0.40	1.22	1.12	0.64
TOM1	0.47	0.57	4.99	36.76*	4.66
TOM2	0.70	0.55	0.83	1.38	0.59
TOM3	0.64	0.47*	0.71	0.74	0.51
TOM3_Homologon	0.91	1.13	9.38	63.56*	7.78
YSL2	0.71	0.34	8.63	39.40*	5.98
YSL6	0.64	0.47*	0.71	0.74	0.51
YSL8	0.64	0.62	0.84	0.66	0.77
YSL13	0.64	0.47*	0.71	0.74	0.51
YSL15	1.18	1.25	137.19*	155.42*	101.83*
YSL16	0.40	0.27	0.90	0.82	0.41
	Minus Si		Plus Si		

Figure 6. Regulation of Fe homeostasis-related genes in rice roots as affected by Fe concentration and Fe form grown without Si and with Si (3 and $30\,mg\,Si\,L^{-1}$, respectively) in nutrient solution. The $2^{-\Delta\Delta Ct}$ values against the control are shown. (**A**) Gene expression in roots of rice plants grown with Fe^{EDDHA} in various concentrations (control = −Si, $2\,mg\,L^{-1}$ Fe). (**B**) Gene expression in roots of rice plants grown with 2 mg Fe in the form of Fe^{EDDHA}, Fe^{EDTA} and Fe$^{(II)}$SO$_4$ (control = −Si, Fe^{EDDHA}). A star indicates significant differences against the control. Green color indicates downregulation and a red color upregulation compared to the WT grown without Si at optimal Fe conditions ($2\,mg\,L^{-1}$ Fe^{EDDHA}).

the aerenchyma into the rhizosphere of rice roots[5,6,47–49]. Furthermore, it was observed that Si reduces sodium uptake in rice due to a reduced transpirational bypass flow[17,18]. However, the impact of exodermal CBs in nutrient and water uptake is controversially discussed in the literature. Apoplastic tracers are shown to be permeable in roots with an exodermis, such as trisodium 3-hydroxy-5,8,10-PTS or *cis*-ABA[10,15]. However, it is discussed that
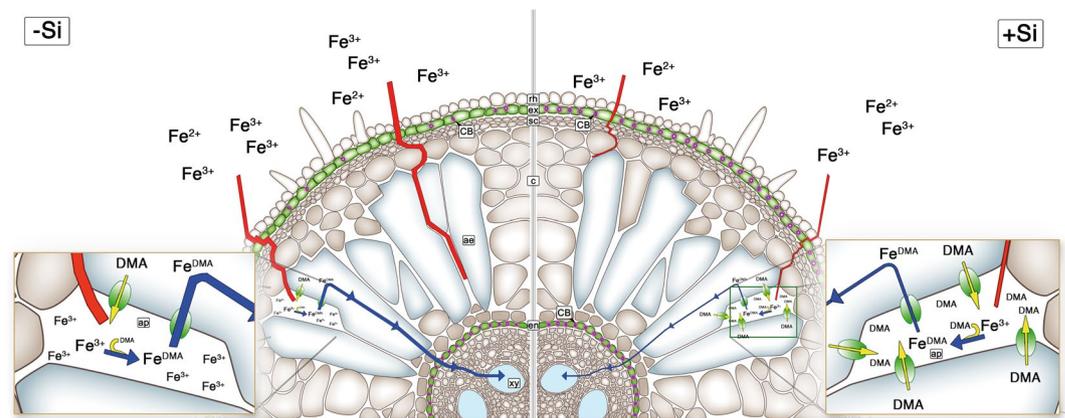
Figure 7. The Fe acquisition in rice roots grown in nutrient solution as affected by Si supply. Without Si supply, the Fe flux into the apoplast of the cortex is not severely restricted by CB in the exodermis. In the apoplast of the cortex Fe binds to excreted DMA and is taken up into the cortex cells and passes the endodermis symplastically into the xylem. Silicon supply induces the CB formation in the exodermis and hampers the flux of Fe into the apoplastic space where less Fe can be bound to DMA resulting in a reduced symplastic flux into the xylem. Abbreviations are rh: rhizodermis, ex: exodermis, sc: sclerenchyma, CB: Casparian band, c: cortex, ae: aerenchyma, ap: apoplast, en: endodermis, xy: xylem. Red and blue lines indicate apoplastic and symplastic flux, respectively.

the lateral root formation may interrupt the exodermal CBs, resulting in a reduced barrier function of the exodermis[8,50]. Earlier results from Hinrichs *et al.*[27] suggested the exodermal CBs as a diffusion barrier for Fe into the apoplastic space. We observed that Si supply reduced the concentration of apoplastic Fe (Fig. 4), supporting the evidence that CBs act as a barrier for the flux of Fe into the root cortex. The apoplastic Fe concentration was in the range of 46 up to 99 μg g FW^{-1} (1–2 μmol g FW^{-1}) at optimal Fe conditions, as observed in other studies[51]. Furthermore, a mutant overexpressing the ABC transporter Os*ABCG25* resulting in enhanced CB development[27] also had a decreased concentration of Fe in the shoot DM (Fig. 5). The presented results support the hypothesis that the exodermal CBs hamper the flux of Fe from the nutrient solution into the apoplast of the root cortex.

Rice is a strategy II plant[52], releasing DMA by transporters into the rhizosphere of plants grown in soil where DMA binds to Fe ions. The Fe-loaded DMA is taken up into the symplast by transporters located in the root epidermis and in the cortex. Regarding plants grown in nutrient solution, however, the whole solution volume can be considered as rhizosphere because of the large diffusion coefficient and the DMA secreted will be extremely diluted and less effective for Fe acquisition. Thus, it was further suggested that under these conditions, the uptake of Fe most probably takes place from the apoplast where the excreted DMA binds to Fe and then the complex is taken up into the cortex cells[42].

A scheme displaying the suggested functions of Si in Fe acquisition of plants grown in nutrient solution is presented in Fig. 7. The Si-induced CB formation in the exodermis hampers the flow of Fe into the apoplastic space where less Fe can be bound to DMA and taken up into the symplast. In agreement with this model, Si supply induced upregulation of Fe homeostasis genes. This proposed mechanism of Si function is in line with the apoplastic obstructuion hypothesis as working model to understand the role of Si in plant biology[7]. One premise of this model is that there is no biochemical role for $Si(OH)_4$ in terms of interactions with enzymes or other intracellular constituents but that such reactions are based on indirect effects caused by Si deposition and reactions in the apoplast. In a certain way this agrees with a lack of specifity of Si-transporters which originate according to the horizontal gene transfer model from bacterial As-transporters[2].

The Si-induced reduction of Fe uptake was also reflected in gene expression. The transcriptomic data displayed the full range of Fe deficiency-induced reaction cascade in rice (Figs. 1 and 6). An overview of the interacting genes and their activity sites is given in Fig. 8. The reaction cascade starts with the transcription factors Os*IDEF1* or 2, which both are regulating elements of Os*TOM1*, Os*IRO2*, Os*NAS1* +2, Os*NAAT1* and Os*DMAS*. But not Os*NAS3* which is only active under excess Fe conditions[53]. The transcript level of Os*IDEF1* +2 is not influenced by Fe availability, but only the protein binding to the DNA is enhanced during Fe deficiency[40,54]. This agrees well with our results that Si did not affect their expression levels (Fig. 6). The activity of Os*HRZ1* is enhanced by IDEF1 and is suggested as negative feedback loop[55]. Putatively, Os*IRO2* activates the biosynthesis of NA and, thus, the synthesis of DMA and MA in subcellular organelles through Os*NAS1*, Os*NAS2*, Os*NAAT1* and Os*DMAS*[39]. The DMA is then transported via OsTOM1 into the apoplast[30,40].

TOM3 was not affected by Si in rice roots, while the TOM3 homologon (*Os12g0132500*) was highly upregulated, which agrees with the literature[35]. An upregulation of the TOM3 homologon was found, but not of Os*TOM3* in the epidermis of rice roots in Fe-deficient conditions.

The putative vacuole transporter Os*ENA1*[40] transporting NA was upregulated. Os*ENA1* is thought to mobilize Fe during Fe shortage from the vacuole. Further characterization of Os*ENA1* is necessary, since the recent research is only based on *in vitro* motif predictions. Finally, Fe-loaded DMA is taken up by different YSL transporters. Os*YSL2* is described as expressed mainly in phloem companion cells for the transport of Fe^{II}-NA[34].
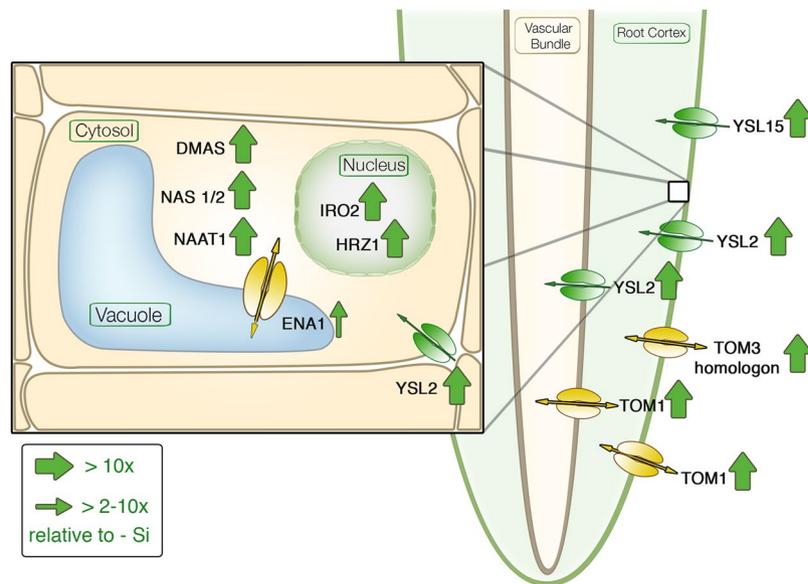
Figure 8. Schematic figure of Si-induced Fe homeostasis-related genes in rice displaying the function of significantly regulated genes from Fig. 6. A big arrow indicates an upregulation compared to the control (−Si; plants grown without Si) with a minimum of tenfold; a small arrow indicates an upregulation with a minimum of twofold. Please see Fig. 1 for abbreviations.

Because of the Si-induced shortage of Fe, Os*YSL2* was highly upregulated. Most probably, Os*YSL2* is responsible for the uptake and distribution of Fe^{II}-NA by Si-induced Fe shortage. No regulation was observed for Os*YSL9* and Os*YSL13*. Os*YSL9* was recently shown to be expressed in the cortical cells of roots[36] and Os*YSL13* was described in cortex and epidermis cells[35]. Both, Os*YSL9* and *13* transporters do not seem to be involved in the Si-dependent reaction. Os*YSL15* was highly upregulated, but not Os*YSL16*; both are located in the exodermis or in the cortex. Os*YSL15*, transporting Fe^{III}DMA, is under Fe deficiency induced in all root parts[56].

Beneficial effects of Si supply on Fe stress alleviation in barley are reported by Nikolic *et al.*[56]. On the first glance, this seems to be in contrast to our results. However we investigated the Fe uptake from nutrient solution whereas Nikolic *et al.* studied the mobilization of Fe in plants after transfer to -Fe conditions.

Conclusion

Silicic acid supply in nutrient solution stimulates the formation of exodermal CBs. It is suggested that this barrier reduced the flux of Fe into the apoplastic space where less Fe was available for chelation by DMA and plant uptake. The plant reacted with an upregulation of Fe homeostasis-related genes and a higher production of Fe-chelating substances as a metabolic answer to the Fe shortage. This response was not sufficient to overcome the Si effect, since shoot Fe concentration was still decreased. This Si role might be specific for rice grown in nutrient solution, because binding of Fe to DMA is discussed to occur in the root apoplast since the excreted DMA is extremely diluted in the nutrient solution compared to the situation soil.

Material and methods

Plant material, growth conditions and harvest. Seeds of *Oryza sativa ssp. Japonica* cv. Selenio were first surface sterilized in 70% ethanol for 1 min and then for 30 min in 3.5% NaClO, followed by washing in sterile water three times. Germination was carried out for several days between two layers of filter paper standing in sterile tap water for 14 d. Seedlings were transferred to non-aerated nutrient solution in 5-L pots containing 0.43 mM NH_4NO_3, 0.32 mM $NaH_2PO_4 \times 2 \times H_2O$, 0.51 mM K_2SO_4, 1 mM $Ca(NO_3)_2 \times 4 \times H_2O$, 1.6 mM $MgSO_4 \times 7 \times H_2O$, 1.82 μM $MnSO_4 \times H_2O$, 0.03 μM $(NH_4)_6Mo_7O_{24} \times 4 \times H_2O$, 9 μM H_3BO_3, 0.6 μM $ZnSO_4 \times 7 \times H_2O$ and 0.15 μM $CuSO_4 \times 5 \times H_2O$. Iron was added as Sequestren™ (Fe^{EDDHA}, Syngenta Agro GmbH, Maintal, Germany) for Fe gradient experiment in three different levels, low Fe (3.58 μM Fe^{EDDHA}), optimal Fe (35.81 μM Fe^{EDDHA}) and high Fe (179.05 μM Fe^{EDDHA}) corresponding to 0.2, 2 and 10 mg Fe, respectively, in nutrient solution. An amount of 2 mg Fe L^{-1} was added as Fe^{EDDHA}, Fetrilon™ (Fe^{EDTA}, BASF, Ludwigshafen, Germany) and iron sulfate ($Fe^{II}SO_4 \times 7 \times H_2O$, CAS: 7782-63-0, KMF, Lohmar, Germany) for the Fe form experiments. Plants were cultivated for three weeks as in the Fe gradient experiment, and the last week with 4.475 mM Fe supplied as $Fe^{II}SO_4 \times 7 \times H_2O$ for the growth of the mutants of Os*ABCG25*. Please see Hinrichs *et al.*[27] for characterization of Os*ABCG25*. The Si was applied as silica gel (SiO_2, Carl Roth, Karslruhe, Germany). A stock solution was prepared by addition of 5 kg silica gel in 1000 L $H_2O^{dest.}$ at RT in the dark. The silica gel dissolved slowly until a Si-concentration of 50 mg*l^{-1} was reached. This stock solution was diluted with $H_2O^{dest.}$ to a working-solution of 30 mg*l^{-1} according to Fleck *et al.*[6]. The $H_2O^{dest.}$ had a basal Si-concentration of 3 mg*l^{-1} due to technical reasons. The resulting Si concentrations in the plant are in the range of 0.1 and 60 mg g^{-1} shoot DM according to previous findings[57]. The pH value of the nutrient solution was adjusted to 6.0 by the addition of 10% H_2SO_4 or 5 M KOH. The nutrient solution was renewed weekly for the first two weeks, after two weeks, and subsequently the nutrient

solution was changed twice a week until harvest. Plants were cultivated in a climate chamber (photoperiod 16/8 h light/dark; temperature, 25/20 °C day/night; 75% relative humidity and a light intensity of 220 µmol m^{-2} s^{-1}) for 28 d in nutrient solution.

After 28 d in nutrient solution, the root zones 4–6 cm from the the root tip were harvested, transferred immediately to liquid nitrogen and stored at -80 °C for transcript analysis. Only adventitious roots were harvested for Fe determination in the apoplast. Shoot and root were separated, dried at 60 °C for 4 d and ground for element analysis. The content of chlorophyll was measured spectrometrically using an N-Tester (Yara, Dülmen, Germany).

Fe determination apoplast.   Adventitious roots were separated and Fe on the root surface was removed through rinsing in anaerobe washing solution (12 mM $Na_2S_2O_4$, 10 mM MES, 0.5 mM $Ca(NO_3)_2$, pH $= 5.5$) for 5 s. Subsequently, the roots were washed three times in H_2O and transferred into 21 ml anaerobe reaction solution (1.5 mM 2.2-Bipyridyl, 10 mM MES, 0.5 mM $Ca(NO_3)_2$, pH $= 5.5$)[51]. The reaction solution with the samples was deoxygenized by N_2 bubbling in an Erlenmeyer flask covered with a cotton plug for 2 min. After 2 min, 1 ml of a cooled 250 mM $Na_2S_2O_4$-solution was added using a syringe and incubated by gently shaking for 5 min at room temperature. After incubation, the roots were removed, and the reaction was stopped. The washing solution and reaction solution were stored on ice with constant N_2-bubbling until usage. The Fe was determined by measuring the A520 of the filtrated reaction solution.

Transcript analysis.   Frozen root material was ground under liquid nitrogen and the RNA was isolated using NucleoSpin RNA Plant (Macherey-Nagel, Düren, Germany), following the manufacturer's instructions. The RNA quality was determined electrophoretically by 1% Agarosegel and fluoretically using a Nanophotometer (Implen, Munich, Germany). The RNA (1 µg), oligo(dT)18-Primer (0.25 µg) and random hexamer primer (0.25 µg) were used to synthesize first-strand cDNA using the Revert Aid™ H Minus First Strand cDNA Synthesis Kit (Fermentas, St. Leon-Rot, Germany), following the manufacturer's instructions for GC-rich templates.

The RNA was additionally measured by capillary electrophometric by a bioanalyzer (Agilent 2100 bioanalyzer, Agilent Technologies) using a RNA 6000 nano assay in the GeneChip experiment. Only samples with a RNA integrity number over 9.5 were used for the GeneChip experiment. A set of sixteen Genechips were used for the experiment, consisting of two treatments (+Si/−Si), four biological repeats and two technical repeats of the Affymetrix GeneChip experiment. One biological repeat consisted of a pool of the RNA of five plants grown in the same 5-L pot.

An amount of 50 ng cDNA was used as a template in 10 µl reaction mix of the SYBR Premix Ex Taq (Tli RNase H Plus) (Takara Bio Europe SAS, Saint-Germainen-Laye, France) and 0.2 µM forward and reverse primer in the quantitative real time PCR (qRT-PCR) experiments. The qRT-PCR runs were performed in the CFX96 cycler (Bio-Rad, München, Germany), using an initial 95 °C step for 30 s, followed by 40 cycles of 95 °C for 5 s, and 60 °C for 30 s, and a final melting curve procedure with a stepwise increment of 0.5 °C ranging from 65 to 95 °C.

The eukaryotic elongation factor 1-alpha (eF1-α, LOC_Os03g08020.1) and Ubiquitin-40S ribosomal protein S27a-1 (UBQ5, LOC_Os01g22490) were used as an endogenous control due to its stable transcript abundance in rice[58,59]. The geometric mean of the Ct values of the two endogenous control genes was calculated according to the literature[60], and this was used to calculate the foldover reference of the different samples (2-delta Ct). A list of primer sequences used can be found in Supplementary Table S1. The primer was tested for specificity in a ten times dilution series starting with 50 ng cDNA and then sequencing of the PCR product. Three technical and four biological replicates were used for each target in qRT-PCR. The relative quantity was calculated using the R-Macro "qpcrmix"[61], based on the $2^{-\Delta\Delta CT}$ method.

Chemical analysis.   For the determination of the Si concentrations in the shoot and root, 200 mg dried plant matter was digested in 3 ml 65% HNO_3, 2 ml H2O and 2 ml 30% H_2O_2 in a microwave for 12 min at 190 °C, then diluted with 20 ml 10% NaOH, neutralized with HNO_3[62] and filled up to a final volume of 100 ml.

In order to determine the Fe, 50 mg of dried and ground shoot matter was digested in 2 ml 65% HNO_3, 2 ml H_2O and 0.5 ml 30% H_2O_2 in a microwave for 25 min at 190 °C and then diluted with distilled water to 25 ml.

The Si and Fe concentrations in the plant extracts and nutrient solutions- were measured by ICP-MS (7500c Agilent Technologies).

Zeta potential measurements.   The hydrodynamic particle size of possible precipitates of the elements Si and Fe in the nutrient solution was determined by the Zeta potential analyzer with light scattering technique (ZetaPALS, Brookhaven, Holtsville,NY, USA)[63]. Freshly prepared nutrient solution without Fe and with Si and nutrient solution with Fe^{EDDHA} with and without Si were measured immediately or incubated for three and seven days in the same conditions as used for growth of rice in the dark. An aliquot of 1.6 ml was transferred in a cuvette and measurement was performed with ten runs each partitioned in 20 cycles, whereby the mean is represented in the figure.

Statistical analysis.   All treatments were replicated four times unless stated otherwise and the mean of the treatments were compared using t-test, Tukey or Bonferroni test utilizing Sigma Plot (Systat Software Inc., San Jose, USA). The statistical qRT-PCR analysis was performed using the R-Macro of Steibel et al.[61]. A students t-test was used with unpaired correlated p-Value for the raw Affymetrix GeneChip data using "GeneSpring" Software (Version 12.0, Agilent). A ranking of candidates was carried out using the "Omics Explorer" (Version 3, Qulcore).

The Affymetrix experiment, including the RNA quality control, GeneChip hybridization, normalization with GeneSpring Software and ranking with the Omics Explorer, was carried out by Dr. Dittrich-Breiholz at the Research Core Unit "Transcriptomics," Institute of Cell Biochemistry, Hannover Medical School.

References

1. Epstein, E. Silicon. *Annu. Rev. Plant Physiol.* 641–64 (1999).
2. Pommerrenig, B. *et al*. Functional evolution of Nodulin26-like Intrinsic Proteins: From bacterial arsenic detoxification to plant nutrient transport. *New Phytologist*, https://doi.org/10.1111/nph.16217 (2019).
3. Ma, J. F., Miyake, Y. & Takahashi, E. Silicon as a beneficial element for crop plants. in Studies in Plant Science (eds. Datnoff, L. D., Snyder, G. H. & G.H., K.) 8, 17–39 (Elsevier B.V., 2001).
4. Ma, J. F. & Yamaji, N. Functions and transport of silicon in plants. *Cell. Mol. Life Sci.* **65**, 3049–57 (2008).
5. Vaculík, M., Lux, A., Luxová, M., Tanimoto, E. & Lichtscheidl, I. Silicon mitigates cadmium inhibitory effects in young maize plants. *Environ. Exp. Bot.* **67**, 52–58 (2009).
6. Fleck, A. T. *et al*. Silicon enhances suberization and lignification in roots of rice (Oryza sativa). *J. Exp. Bot.* **62**, 2001–11 (2011).
7. Coskun, D. *et al*. The controversies of silicon's role in plant biology. *New Phytol.* **221**, 67–85 (2019).
8. Ma, F. & Peterson, C. A. Current insights into the development, structure, and chemistry of the endodermis and exodermis of roots. *Can. J. Bot.* **81**, 991 (2003).
9. Schreiber, L., Franke, R., Hartmann, K.-D., Ranathunge, K. & Steudle, E. The chemical composition of suberin in apoplastic barriers affects radial hydraulic conductivity differently in the roots of rice (Oryza sativa L. cv. IR64) and corn (Zea mays L. cv. Helix). *J. Exp. Bot.* **56**, 1427–1436 (2005).
10. Zimmermann, H. M. & Steudle, E. Apoplastic transport across young maize roots: Effect of the exodermis. *Planta* **206**, 7–19 (1998).
11. Armstrong, W. Radial Oxygen Losses from Intact Rice Roots as Affected by Distance from the Apex, Respiration and Waterlogging. *Physiologia Plantarum* **25**, 192–197 (1971).
12. Steudle, E. Water uptake by roots: an integration of views. *Plant Soil* **226**, 45–56 (2000).
13. Enstone, D. E. & Peterson, C. A. Suberin deposition and band plasmolysis in the corn (Zea mays L.) root exodermis. *Can. J. Bot.* **75**, 1188–1199 (1997).
14. Sattelmacher, B. The apoplast and its significance for plant mineral nutrition. *New Phytol.* **149**, 167–192 (2001).
15. Freundl, E., Steudle, E. & Hartung, W. Apoplastic transport of abscisic acid through roots of maize: effect of the exodermis. *Planta* **210**, 222–231 (2000).
16. Gierth, M., Stelzer, R. & Lehmann, H. An analytical microscopical study on the role of the exodermis in apoplastic Rb+ (K+) transport in barley roots. *Plant Soil* **207**, 209–218 (1999).
17. Yeo, A. R. *et al*. Silicon reduces sodium uptake in rice (Oryza sativa L.) in saline conditions and this is accounted for by a reduction in the transpirational bypass flow. *Plant, Cell Environ.* **22**, 559–565 (1999).
18. Gong, H. J., Randall, D. P. & Flowers, T. J. Silicon deposition in the root reduces sodium uptake in rice (Oryza sativa L.) seedlings by reducing bypass flow. *Plant. Cell Environ.* **29**, 1970–1979 (2006).
19. Faiyue, B., Al-Azzawi, M. J. & Flowers, T. J. The role of lateral roots in bypass flow in rice (Oryza sativa L.). *Plant, Cell Environ.* **33**, 702–716 (2010).
20. Stasovski, E. & Peterson, C. A. The effects of drought and subsequent rehydration on the structure, vitality, and permeability of Allium cepa adventitous roots. *Can. J. Bot.* **69**, 1170–1178 (1991).
21. Kamula, S. A., Peterson, C. A. & Mayfield, C. I. The plasmalemma surface area exposed to the soil solution is markedly reduced by maturation and death of the epidermis and death of the exodermis in onion roots. *Plant. Cell Environ.* **17**, 1183–1193 (1994).
22. Garcia, A. *et al*. Sodium and potassium transport to the xylem are inherited independently in rice, and the mechanism of sodium: Potassium selectivity differs between rice and wheat. *Plant Cell Environ.* **20**, 1167–1174 (1997).
23. Ma, J., Goto, S., Tamai, K. & Ichii, M. Role of root hairs and lateral roots in silicon uptake by rice. *Plant Physiol.* **127**, 1773–1780 (2001).
24. Flam-Shepherd, R. *et al*. Membrane fluxes, bypass flows, and sodium stress in rice: The influence of silicon. *J. Exp. Bot.* **69**, 1679–1692 (2018).
25. Nishiuchi, S., Yamauchi, T., Takahashi, H., Kotula, L. & Nakazono, M. Mechanisms for coping with submergence and waterlogging in rice. *Rice* **5**, 2 (2012).
26. Leite, D. C. C. *et al*. Cell wall changes during the formation of aerenchyma in sugarcane roots. *Ann. Bot.* **120**, 693–708 (2017).
27. Hinrichs, M. *et al*. An ABC Transporter Is Involved in the Silicon-Induced Formation of Casparian Bands in the Exodermis of Rice. *Front. Plant Sci.* **8**, 671 (2017).
28. Fleck, A. T. *et al*. Silicon promotes exodermal casparian band formation in Si-accumulating and Si-excluding species by forming phenol complexes. *PLoS One* **10**, e0138555 (2015).
29. Ma, J. F. & Takahashi, E. Effect of silicon on the growth and phosphorus uptake of rice. *Plant Soil* **126**, 115–119 (1990).
30. Nozoye, T. *et al*. Nicotianamine synthase 2 localizes to the vesicles of iron-deficient rice roots, and its mutation in the YXXφ or LL motif causes the disruption of vesicle formation or movement in rice. *Plant J.* **77**, 246–260 (2014).
31. Marschner, H. & Römheld, V. Strategies of plants for acquisition of iron. *Plant Soil* **165**, 261–274 (1994).
32. Schmid, N. B. *et al*. Feruloyl-CoA 6'-Hydroxylase1-Dependent Coumarins Mediate Iron Acquisition from Alkaline Substrates in Arabidopsis. *Plant Physiol.* **164**, 160–172 (2014).
33. Mori, S. & Nishizawa, N. Methionine as a Dominant Precursor of Phytosiderophores in Graminaceae Plants. *Plant Cell Physiol.* **28**, 1081–1092 (1987).
34. Koike, S. *et al*. OsYSL2 is a rice metal-nicotianamine transporter that is regulated by iron and expressed in the phloem. *Plant J.* **39**, 415–424 (2004).
35. Ogo, Y. *et al*. Tissue-specific transcriptional profiling of iron-deficient and cadmium-stressed rice using laser capture microdissection. *Plant Signal Behav* **9**, e29427 (2014).
36. Senoura, T. *et al*. The iron-chelate transporter OsYSL9 plays a role in iron distribution in developing rice grains. *Plant Mol. Biol.* **95**, 375–387 (2017).
37. Higuchi, K., Kanazawa, K., Nishizawa, N. K., Chino, M. & Mori, S. Purification and characterization of nicotianamine synthase from Fe-deficient barley roots. *Plant Soil* **165**, 173–179 (1994).
38. Shojima, S. *et al*. Biosynthesis of Phytosiderophores. *Plant Physiol.* **93**, 1497–1503 (1990).
39. Bashir, K. & Nishizawa, N. K. Deoxymugineic Acid Synthase. *Plant Signal. Behav.* **1**, 290–292 (2006).
40. Nozoye, T. *et al*. Phytosiderophore efflux transporters are crucial for iron acquisition in graminaceous plants. *J. Biol. Chem.* **286**, 5446–5454 (2011).
41. Ogo, Y. *et al*. patial transcriptomes of iron-deficient and cadmium-stressed rice. *New Phytol.* **201**, 781–794 (2014).
42. Zhang, F. S., Römheld, V. & Marschner, H. Role of the root apoplasm for iron acquisition by wheat plants. *Plant Physiol.* **97**, 1302–1305 (1991).
43. Marschner's Mineral Nutrition of Higher Plants (Third Edition) (ed. Marschner, P.) 347–368 (Academic Press, 2012), https://doi.org/10.1016/B978-0-12-384905-2.00014-5.

44. Dufey, I., Gheysens, S., Ingabire, A., Lutts, S. & Bertin, P. Silicon Application in Cultivated Rices (Oryza sativa L. and Oryza glaberrima Steud.) Alleviates Iron Toxicity Symptoms Through the Reduction in Iron Concentration in the Leaf Tissue. *J. Agron. Crop Sci.*, https://doi.org/10.1111/jac.12046 (2013).

45. Yadav, R., Flowers, T. J. & Yeo, A. The involvement of the transpirational bypass flow in sodium uptake by high- and low-sodium-transporting lines of rice developed through intravarietal selection. *Plant, Cell Environ.* **19**, 329–336 (1996).

46. Ranathunge, K., Steudle, E. & Lafitte, R. Control of water uptake by rice (Oryza sativa L.): role of the outer part of the root. *Planta* **217**, 193–205 (2003).

47. Kolattukudy, P. E. & Agrawal, V. P. Structure and composition of aliphatic constituents of potato tuber skin (suberin). *Lipids* **9**, 682–691 (1974).

48. Schreiber, L., Franke, R., Hartmann, K. D., Ranathunge, K. & Steudle, E. The chemical composition of suberin in apoplastic barriers affects radial hydraulic conductivity differently in the roots of rice (Oryza sativa L. cv. IR64) and corn (Zea mays L. cv. Helix). *J. Exp. Bot.* **56**, 1427–1436 (2005).

49. Colmer, T. D. & Bloom, A. J. A comparison of NH4+ and NO3- net fluxes along roots of rice and maize. *Plant, Cell Environ.* **21**, 240–246 (1998).

50. Ranathunge, K., Steudle, E. & Lafitte, R. Blockage of apoplastic bypass-flow of water in rice roots by insoluble salt precipitates analogous to a Pfeffer cell. *Plant, Cell Environ.* **28**, 121–133 (2005).

51. Bienfait, H. F., van den Briel, W. & Mesland-Mul, N. T. Free space iron pools in roots: generation and mobilization. *Plant Physiol.* **78**, 596–600 (1985).

52. Römheld, V. & Marschner, H. Evidence for a specific uptake system for iron phytosiderophores in roots of grasses. *Plant Physiol.* 175–180, https://doi.org/10.1104/pp.80.1.175 (1986).

53. Aung, M. S. *et al*. Nicotianamine synthesis by OsNAS3 is important for mitigating iron excess stress in rice. *Front. Plant Sci.* **10**, 1–16 (2019).

54. Kobayashi, T. & Nishizawa, N. K. Iron sensors and signals in response to iron deficiency. *Plant Science* **224**, 36–43 (2014).

55. Kobayashi, T. *et al*. Iron-binding haemerythrin RING ubiquitin ligases regulate plant iron responses and accumulation. *Nat. Commun.* **4**, 1–12 (2013).

56. Nikolic, D.B. *et al*. Silicon Alleviates Iron Deficiency in Barley by Enhancing Expression of Strategy II Genes and Metal Redistribution. *Frontiers in Plant Science*., https://doi.org/10.3389/fpls.2019.00416 (2019).

57. Fleck, A. Silicon Effects on Arsenic Uptake in Rice, Exodermis Development and Expression of Genes Related to Suberin and Lignin Metabolism (2013).

58. Jain, M., Nijhawan, A., Tyagi, A. K. & Khurana, J. P. Validation of housekeeping genes as internal control for studying gene expression in rice by quantitative real-time PCR. *Biochem. Biophys. Res. Commun.* **345**, 646–51 (2006).

59. Jain, M. Genome-wide identification of novel internal control genes for normalization of gene expression during various stages of development in rice. *Plant Sci.* **176**, 702–706 (2009).

60. Vandesompele, J. *et al*. Accurate normalization of real-time quantitative RT-PCR data by geometric averaging of multiple internal control genes. *Genome Biol.* **3**, 34–1 (2002).

61. Steibel, J. P., Poletto, R., Coussens, P. M. & Rosa, G. J. M. A powerful and flexible linear mixed model framework for the analysis of relative quantification RT-PCR data. *Genomics* **94**, 146–152 (2009).

62. Haysom, M. B. & Ostatek-Boczynski, Z. A. Rapid, wet oxidation procedure for the estimation of silicon in plant tissue. *Commun. Soil Sci. Plant Anal.* **37**, 2299–2306 (2006).

63. Dultz, S., Woche, S. K., Mikutta, R., Schrapel, M. & Guggenberger, G. Size and charge constraints in microaggregation: Model experiments with mineral particle size fractions. *Appl. Clay Sci.* **170**, 29–40 (2019).

Acknowledgements

Author contributions

Conceived and designed the experiment: M.B and M.K.A.S. Performed the experiments: M.B and N.S.N. Contributed reagents/material/analysis tools: M.K.A.S. Wrote the paper: M.B and M.K.A.S. All authors reviewed the manuscript.

Competing interests

The authors declare no competing interests.

Additional information

Supplementary information is available for this paper at https://doi.org/10.1038/s41598-020-61718-4.

Correspondence and requests for materials should be addressed to M.B.

Reprints and permissions information is available at www.nature.com/reprints.

Publisher's note Springer Nature remains neutral with regard to jurisdictional claims in published maps and institutional affiliations.